This manuscript is a minor revision of an earlier preprint and has been re-submitted for publication in **Frontiers in Earth Science**. It is our expectation that **it will hopefully be accepted for publication**. Subsequent versions of this manuscript may differ due to editorial process. If accepted for publication, the final version will be available through the "Peer-reviewed publication DOI" link on EarthArXiv.

We hope you find this paper interesting and would welcome your feedback on it. Kindly contact Folarin Kolawole (*folarin.kol@gmail.com*) with your feedback.

Structural Inheritance Controls Strain Distribution During Early Continental Rifting, Rukwa Rift

Folarin Kolawole[1,2*], Thomas B. Phillips[3], Estella A. Atekwana[4] and Christopher A-L. Jackson[5]

[1]School of Geosciences, University of Oklahoma, 100 East Boyd Street, RM 710, Norman, Oklahoma 73019

[2]Now at BP America, 501 Westlake Park Blvd, Houston, TX 77079

[3]Department of Earth Sciences, Durham University, Science Labs, Durham DH1 3LE

[4]Department of Earth Science, University of Delaware, 101 Penny Hall, Newark, Delaware 19718

[5]Department of Earth and Environmental Sciences, The University of Manchester, Williamson Building, Oxford Road, Manchester, M13 9PL, UK

*Corresponding Author: F. Kolawole (folarin.kol@gmail.com)

ABSTRACT

Little is known about rift kinematics and strain distribution during the earliest phase of extension due to the deep burial of the pre-rift and earliest rift structures beneath younger, rift-related deposits. Yet, this exact phase of basin development ultimately sets the stage for the location of continental plate divergence and breakup. Here, we investigate the structure and strain distribution in the multiphase Late Paleozoic-Cenozoic magma-poor Rukwa Rift, East Africa during the earliest phase of extension. We utilize aeromagnetic data that image the Precambrian Chisi Shear Zone (CSZ) and bounding terranes, and interpretations of 2-D seismic reflection data to show that, during the earliest rift phase (Permo-Triassic 'Karoo'): (1) the rift was defined by the Lupa Fault, which exploited colinear basement terrane boundaries, and a prominent intra-basinal fault cluster (329° ±9.6) that trends parallel to and whose location was controlled by the CSZ (326°); (2) extensional strain in the NW section of the rift was accommodated by both the intra-basinal fault cluster and the border fault, where the intra-basinal faulting account for up to 64% of extension; in the SE where the CSZ is absent, strain is primarily focused on the Lupa Fault. The early-rift strain in the Rukwa Rift is thus, not accommodated only by border the fault as suggested by

existing magma-poor early-rift models; instead, strain focuses relatively quickly on a large border fault and intra-basinal fault clusters that follow pre-existing intra-basement structures; (3) two styles of early-phase strain localization are evident, in which strain is localized onto a narrow discrete zone of basement weakness in the form of a large rift fault (Style-1 localization), and onto a broader discrete zone of basement weakness in the form of a fault cluster (Style-2 localization). We argue that the CSZ and adjacent terrane boundaries represent zones of basement mechanical weakness that controlled the first-order strain distribution and rift development during the earliest phase of extension. The established early-rift structure, modulated by structural inheritance, then persisted through the subsequent phases of rifting. The results of our study, in a juvenile, and relatively well-exposed and data-rich rift, are applicable to understanding the structural evolution of deeper, buried ancient rifts.

Keywords: Continental Rifting, Tectonic Strain, Normal Faults, Rukwa Rift, Shear Zones, East African Rift System

INTRODUCTION

Tectonic extension of the continental lithosphere is typically accommodated by the brittle deformation of the upper crust, demonstrated by the emergence of normal fault populations (Cowie et al., 2005; Agostini et al., 2011; Muirhead et al., 2016, 2019). Some classic models for the evolution of continental rifts, suggest that during the early phase of extension, strain is initially accommodated by the development of distributed normal faults, with strain subsequently localizing onto a few large faults and subsequently migrating to the rift axis (e.g., Gawthorpe and Leeder, 2000; Cowie et al., 2005; Nixon et al., 2016; Naliboff et al., 2017). However, a comparison of juvenile, magma-rich and magma-poor segments of narrow rifting along the East African Rift System (EARS) show that in contrast to the magma-rich rift basins where strain is accommodated by both the large basin-bounding faults (border faults) and intra-basinal structures, the border faults accommodate most (~90 %) of the strain in the magma-poor rift segment (Muirhead et al., 2019). Elsewhere along the EARS, the incipient (<3 Ma) magma-poor Zomba Graben, southern Malawi Rift, has already witnessed the localization of strain in the rift axis, with the related faults presently accounting for up to 55 % (±24) of the extensional strain (Wedmore et al., 2020). The evidence presented in these studies indicate that early-phase extensional strain along magma-poor continental rifts may or may not be primarily accommodated by only the border faults. Thus, there is a need to better understand other mechanisms that can facilitate early focusing of intra-basinal faulting and extensional strain in magma-poor continental rifts.

Since continental rifts typically develop in previously deformed lithosphere (Wilson, 1966; Dewey and Spall,1975; Buiter and Torsvik, 2014), the distribution of early-phase strain in magma-poor rifts can be complex due to the interaction between faults that exploit or reactivate pre-existing structures, and those that form independently of any pre-existing structure (e.g., Manatschal et al.,

2015; Kolawole et al., 2018; Ragon et al., 2019; Schiffer et al., 2019; Phillips et al., 2019a,b; Heilman et al., 2019; Osagiede et al., 2020; Wang et al., 2021). Overall, very little is known about the earliest phase of continental extension, and even less of how strain is partitioned along inherited structures; this reflects the fact that the associated structures and related stratigraphic record are typically deeply buried beneath younger (i.e., post-rift or later rift phase) sequences and are thus difficult to image with geophysical data, or are overprinted by later tectonic events (e.g., post-rift plate collision). This knowledge gap limits a fuller understanding of the spectrum of processes that govern continental rifting and breakup in space and time.

The EARS (Fig. 1A) is the largest active continental rift system on Earth. This system, which formed by the stretching of previously deformed lithosphere, is characterized by segments that span the major stages of continental rifting from inception to transitional crust (e.g., Daly, 1989; Hayward & Ebinger, 1996; Delvaux, 2001; Ebinger, 2005; Chorowicz, 2005). We integrate available geophysical and geological datasets from the multiphase magma-poor Rukwa Rift (Figs. 1A-B, 2A-D) to explore how strain was distributed during the earliest phase of extension, and investigate the dominant controls. We show that the potentially lithosphere-scale Precambrian Chisi Shear Zone (CSZ) and its adjacent terrane boundaries (Fig. 1B; Lemna et al., 2019; Heilman et al., 2019) represent major zones of pre-rift basement mechanical weakness that controlled the location, structure, and evolution of both the border and intra-basinal faults during the earliest phase of continental extension. We show how the geometry of the CSZ controlled along-rift variations in the early-phase tectonic extension and overall basin geometry, the effects of which persist through and thus influence the later rift geometry. We also expand our analysis to the nearby Luama Rift (located in DRC), which is coeval, colinear with, and parallel to the Rukwa Rift; both basins representing structural elements along a NW-trending Karoo-age rift branch herein referred

to as “the Rukwa Trend" (Fig. 1A). Our results resolve a long-standing controversy related to the geometrical structure and kinematics of rifting in this part of the East African Rift System.

GEOLOGICAL SETTING

The Precambrian (Pre-Rift) Basement of the Rukwa Trend

The crystalline basement of the Rukwa Trend is composed of the metamorphic and igneous rocks of the Precambrian (1.95 -1.85 Ga) Ubendian Belt, which formed during the collision of the Archean Tanzania Craton and the Bangweulu Block, and which comprises the Ufipa, Katuma, Wakole, Lupa, Mbozi, Ubende, and Upangwa terranes (Figs. 1A-B; Daly, 1988; Lenoir et al., 1994). This orogenic belt, which is defined by several NW-trending terranes (2.1-2.025 Ga) that are bounded by steeply dipping, ductile, amphibolite facies, strike-slip shear zones (Fig. 1B; Daly, 1988; Lenoir et al., 1994; Theunissen et al., 1996; Kolawole et al., 2018). The terranes are composed of amphibolite to granulite facies gneisses with foliations that dominantly trend NW-SE and commonly steepen near the terrane boundaries (Lenoir et al., 1994). Although relative rare compared to gneisses, other metasediments along the belt consists of mica schists, marbles, meta-anorthosites, and ferruginous quartzites (Lenoir et al., 1994).

The geochronology, geochemistry, and metamorphic structure of the Ubendian Belt suggests that it formed in response to multiple episodes of wrench tectonic events (Theunissen et al., 1996) with phases of subduction extending from the Paleoproterozoic to the Neoproterozoic (Ganbat et al., 2021). The orogenic belt first developed during a phase of collisional orogeny along the SW margin of the Tanzanian Craton (ca 2.1 - 2.0 Ga), after which the belt experienced two episodes

of wrench tectonics consisting of an initial phase of dextral strike-slip shear at ca. 1.8 – 2.0 Ga, followed by a ductile-brittle sinistral strike-slip reactivation in the Neoproterozoic (Lenoir et al., 1994). This Neoproterozoic shear reactivation recorded the development of thick mylonite and blastomylonite zones with low-grade metamorphic assemblages along shear zones that bound the terranes. The terranes and associated fabrics which are observable in basement exposures along the flanks of the Phanerozoic Rukwa Rift, are suggested to have exerted some control on the development of the basin (Wheeler and Karson, 1994; Theunissen et al., 1996; Klerkx et al., 1998; Boven et al., 1999; Lemna et al., 2018; Heilman et al., 2019).

The Chisi Shear Zone (CSZ)

Along the Ubendian Belt, the Chisi Shear Zone (CSZ) is a prominent shear zone which separates the Ufipa Terrane to the southwest, from the Wakole and Ubende Terranes to the northeast (Fig. 1B). The structure was initially identified as the "Ikulu series" or "Ikulu Terrane", a broad (6 - 12 km-wide in Chisi area) shear belt composed of amphibolite, micaschist, and meta-calcareous rocks with high pressure blueschist or eclogitic associations (Lenoir et al., 1994; Boven et al., 1999). The mafic high-pressure sequences along the shear zone were interpreted to represent disrupted remnants of deeply subducted ophiolites (Smirnov et al., 1973; Lenoir et al., 1994; Klerkx et al., 1997; Sklyarov et al., 1998).

Along the 'Ikulu' structure, amphibolites and amphibole gneisses exhibit metamorphic foliation with planes that dominantly strike WNW-ESE and dip steeply to the NNE and S-SSW (stereographic plot with red filled circles in Fig. 2A; Theunissen et al., 1996; Boven et al., 1999). The rocks also exhibit mineral elongation lineation and some fold axes of asymmetric intrafolial

folds that generally trend NW-SE and plunge shallowly-to-moderately to the ESE-SE (stereographic plot with open diamonds in Fig. 2A). Mylonitic rocks along the SW margin of the granulitic Ubende Terrane exhibit P-T characteristics and shear fabrics suggesting an uplift and exhumation of the terrane relative to the felsic Ufipa Terrane on the SW flank of the 'Ikulu' structure (Theunissen et al., 1996; Sklyarov et al., 1998; Boven et al., 1999). More detailed petrographic and geochemical investigation of the eclogites reveal striking similarities with oceanic island-arc volcanic rocks (Boniface & Schenk, 2012). Geochronologic analyses indicate a clustering of Paleoproterozoic eclogites to the northern segment of the structure (near Lake Tanganyika) and Neoproterozoic eclogites to the south (e.g., Chisi area and northern Malawi) (Fig. 1B), suggesting multiple cycles of subduction-related orogenic events along the structure (Boniface & Schenk, 2012; Boniface et al., 2012; Ganbat et al., 2021). Thus, the 'Ikulu' domain was proposed to be the primary Late Proterozoic (Pan African Orogeny) suture zone between the Tanzania and Bangweulu Cratons along the Ubendian Belt (Boniface & Schenk, 2012).

Further, the magnetic-high anomaly expression of the 'Ikulu' domain, created by the dominance of mafic rocks along the belt, defines a prominent regional magnetic lineament that extends southeast beneath the Rukwa Rift sedimentary cover, sub-parallel to the northwest trend of the rift (Figs. 1B; Lemna et al., 2019; Heilman et al., 2019). Since the Chisi area of Tanzania represents a type-locality for the detailed studies of the structural fabrics, geochemistry, and petrology of the structure (Theunissen et al., 1996; Boven et al., 1999; Boniface & Schenk, 2012), the structure was recently officially re-introduced as "Chisi Shear Zone" (Lemna et al., 2019) or "Chisi Suture Zone" (Heilman et al., 2019). However, in this current study, we adopt the name "Chisi Shear Zone" to refer to the structure.

Phanerozoic Rifting along the Rukwa Trend

The present-day configuration of the Rukwa Trend consists of multiple colinear, NNW-trending rift basins (Rukwa, Karonga, and Luama basins) that initially developed during Permo-Triassic (Karoo) phase of rifting (e.g., Delvaux, 2001). All three basins were reactivated by extensional tectonics in the Cretaceous (Roberts et al., 2010, 2012). However, only the Rukwa Rift and Karonga Basin (Fig. 1A) experienced significant reactivation in the Cenozoic, and they are still currently active (e.g., Morley et al., 1999; Delvaux, 2001; Chorowicz, 2005). The Rukwa Rift, the primary focus of this study, currently defines a graben and is bounded to the northeast by the Lupa Fault and to the southwest by the Ufipa Fault (Fig. 2B; Heilman et al., 2019; Morley et al., 1999). The basin initially developed as a NE-dipping half graben (with a shallow graben geometry only in the NW) during the Karoo rifting phase, bounded to the northeast by the principal border fault, the Lupa Fault (Figs. 2C-D). The Karoo intra-basinal faults (KIF) and basement highs predominantly trend NNW, oblique to the Lupa Fault strike (Fig. 2B). Estimates of the Karoo-age extension direction vary from NE-SW to E-W (Fig. 2B).

DATASET AND METHODOLOGY

Along the Rukwa Trend, we compile structural mapping and structural measurement data from published 2-D seismic data (e.g., Fig. 2C; Morley et al., 1999) and integrate these with aeromagnetic data (Figs. S1A-B) and satellite radar digital elevation model (DEM) (Figs. S2A-B).

Aeromagnetic Data, Satellite Topographic Data, and their Analyses:

We use aeromagnetic data to map key pre-rift intra-basement structures along the axis of the Rukwa Rift and along-trend of the rift. We applied derivative filters to the aeromagnetic grid to enhance structural features (Fig. 3A), and mathematical transforms to estimate the depths to magnetic sources in the basement (Figs. 3B-D; see supplementary information).

The aeromagnetic data (Fig S1A), collected between 1977-1980 with flight height of 200 m and a flight line spacing of 1 km, was provided by the South African Council for Geoscience. First, we reduced the data to the magnetic pole (RTP) to correct for latitude-dependent skewness (Baranov, 1957), after which we applied a vertical derivative filter to better resolve magnetic gradients associated with structural features (Figs. 3A, S1B) (Salem et al., 2007; Kolawole et al., 2017, 2018; Heilman et al., 2019). In this study, we delineate the boundaries of the Chisi Shear Zone along the edges of the high magnetic anomaly lineament in the vertical derivative map of the aeromagnetic grid. In areas where aeromagnetic data is not available, we augmented the basement mapping with 30 m-resolution Satellite Radar Topographic Mission (SRTM) Digital Elevation Model (DEM) hill shade maps (Figs. S2A-B).

Structural Data from Seismic Interpretation:

We establish the initial (i.e., Karoo rift phase) geometry of the Rukwa Rift and related faults using published seismic reflection profiles, and associated fault trace maps and sediment thickness maps ('Karoo Isopach') presented by Morley et al. (1992, 1999). We also calculate along-rift variations in Karoo-age tectonic extension (backstripped to Karoo time surface; Figs. 4A-D) accommodated by slip on the Lupa Fault and intra-basinal faults, again using data published by Morley et al. (1992). We integrate these structural data with aeromagnetic data analysis to investigate the

influence of the pre-rift basement structure on the early-rift structure and evolution of the Rukwa Rift (Figs. 4A-C).

RESULTS

3-D Geometry and Extent of the CSZ

The petrology and geochemistry, local structure, and topographic expression of the CSZ is well-constrained in the Chisi area, located on the NW flank of the Rukwa Rift (Figs. 1B and 2A; Theunissen et al., 1996 and Boven et al., 1999; Boniface & Schenk, 2012). Field observations show that the CSZ is dominated by steep, NE- and SW-dipping, metamorphic fabrics hosted by eclogite facies rocks (Fig. 2A). At this location, the CSZ is characterized by a prominent NW-trending, positive magnetic anomaly lineament (Fig. 1B) and a topographic ridge (Figs. 2A and S2A). Based on its distinct geophysical and geomorphic expression, as well as known field locations of eclogite rocks, we map the northwestward and southeastward continuations of the CSZ system beneath the Rukwa Rift and along the northeastern boundary zone of the Luama Rift respectively (Fig. 1B).

Northwest of the Chisi area, the CSZ associated structures are colinear with the subaerial Mahale Ridge and the submerged Kavala Island Ridge (submerged beneath Lake Tanganyika), and continues northwest into the Busindi Ridge which itself represents the footwall of the Busindi border fault of the Luama Rift (Fig. 1B, S2A). Along the Luama Rift, the inferred CSZ extension represents the boundary between the Kibaran Belt (to the south) and the Ruzizian Belt to the north (Fig. 1A). Based on the occurrence of a prominent high magnetic lineament extending NNW across Lake Tanganyika from the northernmost known CSZ-related eclogite exposure, a possible

East CSZ splay is delineated to continue northward and link with the N-trending Ubwari Ridge (buried horst and subaerial peninsula; Figs. 1B, S1A-B). Although the Ubwari Ridge is a fault-bounded horst block in the Cenozoic Tanganyika Rift, its possible spatial association with the CSZ inferred based on both the colinearity with the continuation of the magnetic-high anomaly lineament of the CSZ, and the southeastward rotation of the N-trending metamorphic fabrics of the subaerial section of the horst (Figs. S1B and S2B).

The CSZ extends southeastwards from the Chisi area to continue beneath the Rukwa Rift, where it is sub-parallel to the rift border faults (Figs. 1B and 2A). Just southeast of the termination of the CSZ magnetic lineament, the >15 km-wide Mughese Shear Zone (MSZ) which separates the Ufipa and Mbozi Terranes of the Ubendian Belt (Fig. 1B), extends beneath the Msongano Trough (bifurcation of the Rukwa Rift) and continues southeast into the Karonga Basin (Figs. 1B, 2B). Overall, the CSZ-associated aeromagnetic and geomorphic structures extend for >600 km from the Luama and Tanganyika rifts, southeastwards through the Rukwa Rift (Fig. 1B). Although our mapping suggests an along-trend and perhaps genetic relationship between the CSZ and the Mughese Shear Zone (Fig. 1B), we clarify that at the time of this contribution, there is no available data demonstrating that the Mughese Shear Zone is also a subduction-related suture. In the absence of this information, we define the southeast termination of the CSZ as the termination zone of its magnetic anomaly lineament beneath the Rukwa Rift (Figs. 1B and 3A).

Our 3D grid of the depth-distribution of intra-basement magnetic sources along the Rukwa Rift (Figs. 3A-C, S3A-B, S4A-B) reveal a steeply-dipping, NW-trending zone of magnetic sources that extend to 12 km depth; this feature is spatially collocated with the surface trend of the CSZ aeromagnetic lineament (Fig. 3B). Northeast of these CSZ-related magnetic sources, a narrow sub-vertical block of very shallow (<6 km deep) magnetic sources is spatially colocated with the Lupa

Fault. This zone of Lupa Fault-related shallow sources separates the CSZ-related sources from another sub-vertical cluster of moderately deeper (~9 km-deep) magnetic sources that are spatially collocated with the Katuma Terrane (Figs. 3B-D).

The CSZ and the Early-rift (Karoo) Structure

The Karoo-age basin of the Rukwa Rift widens southeastwards from c. 16 km to c. 57 km at the terminus of the CSZ magnetic lineament, before narrowing to <16 km towards the southeast (Fig. 2B). The Karoo intra-basinal faults (KIF, 329°±9.6; Fig. 2Bi) are dominated by a fault cluster, spaced 4-6 km apart and striking oblique to the Lupa Fault (311°). The fault cluster is collocated with the CSZ magnetic lineament and trends parallel to the lineament (Fig. 4A-B). Although, some of the KIF faults dip to the SW, most of them dip to the NE (Fig. 2B). A Karoo isopach map shows that the thickest sections (>1 km-thick) of the Karoo-age units are generally confined to the northeast of the CSZ anomaly (yellow polygon in Fig. 2B; also see Figs. 2C-D). Adjacent to the Katuma Terrane and CSZ lineament (i.e., northwestern half of the rift), the Lupa Fault has a relatively high dip (~69°); this decreases south-eastwards to <40° (Fig. 4C). Also, within the rift, prominent basement ridges cluster along the CSZ, some of which appear to be fault-bounded (Fig. 2B). We note the strong alignment between the CSZ mean trend (326°), KIF mean trend (329°±9.6), and that of all (Permian to Quaternary) rift faults (ARF, 330°; Fig. 2Bii).

Strain Distribution within the Rukwa Rift during Karoo Extension

In the northwestern half of the Rukwa Rift, the proportion of Karoo-phase tectonic extension accommodated by the KIF increased southeastwards from ~12 % to 64 % (Figs. 4C-D). This trend is coincident with an increase in across-strike separation between the Lupa border fault and the CSZ, from <10 km in the NW to ~30 km at the SE terminus of CSZ magnetic lineament (Fig. 4C; see also Fig. 4A). However, southeastward from the CSZ terminus to the southeast tip of the basin, total extension was largely accommodated by the Lupa Fault (up to 83 %; Fig. 4C). Also, NW of the CSZ terminus, the curve for intra-basinal fault absolute extension tracks that of the total absolute extension, whereas SE of the CSZ terminus, total absolute extension curve is not tracked by that of the intra-basinal fault, rather, it is tracked by the Lupa Fault absolute extension (Fig. 4C). The southeastward increase in the percentage of total extension accommodated by the Lupa Fault is consistent with the southeastward increase in the magnitude of Lupa Fault's offset of the Top-Basement which shows a more pronounced increase just southeast of the CSZ terminus (see 'Lupa Fault offset of Top-Basement' curve in Fig. 4C). Northwest of the CSZ terminus, Lupa Fault's offset of the Top-Basement shows a range of 2 - 6.4 km over a distance of 120 km, whereas SE of the CSZ terminus, the basement offset increases from ~5.5 km to >9 km within ~20 km distance.

CONTROLS OF THE CSZ AND TERRANE BOUNDARY ON EARLY-RIFT FAULTING, STRAIN DISTRIBUTION, AND BASIN ARCHITECTURE

Border Fault Development:

The geometrical and spatial relationships between the Karoo rift-related structures, the CSZ, and the adjacent basement terrane boundaries reveal how strain was localized and spatially partitioned

295 during the early phases of extension in the Rukwa Rift. The Lupa Fault is the largest rift-related
296 structure in the Rukwa Rift, having formed at the very onset of rifting, thus representing the border
297 fault (e.g., Morley et al., 1992, 1999; Kilembe and Rosendahl, 1992; Wheeler and Karson 1994).
298 Studies suggest that the Lupa Fault localized along terrane boundaries (Katuma-Wakole boundary
299 in the NW and Lupa-Mbozi boundary in the SE) and that its NW-SE trend is influenced by the
300 structural fabrics in the bounding Katuma Terrane (Figs. 1B, 3B-D; Daly, 1988; Wheeler and
301 Karson, 1994; Theunissen et al., 1996; Lemna et al., 2019; Heilman et al., 2019). However, the
302 observations supporting these hypotheses were based on the shallow geometries of structures
303 observed in the field or the plan-view structural trends of metamorphic fabrics expressed in
304 aeromagnetic data.

305 The sub-vertical dips described by the cluster of magnetic sources beneath the Katuma Terrane
306 (Figs. 3B) supports previous studies that argue that the Katuma-Wakole terrane boundary, and
307 fabrics within the Katuma Terrane, are steeply dipping. However, the Lupa Fault itself shows an
308 abrupt and significant decrease in dip just southeast of the Katuma Terrane termination (Fig. 4C),
309 where it is coincident with the E-W-trending Usagaran Belt and Lupa Terrane (Fig. 5A). Therefore,
310 we suggest that both the Katuma-Wakole Terrane boundary and the tectonic structures in the
311 Katuma Terrane are responsible for the steep dip of the Lupa border fault in the NW; in contrast,
312 to the SE, the absence of favorably oriented intra-basement structures result in the fault having a
313 lower dip.

314 The sub-vertical dip of the CSZ-related magnetic sources and southwest dip direction of the Lupa
315 Fault (Fig. 3C) also suggests that the deepest sections of the border fault could merge with the
316 shear zone at the deeper crustal levels, although it would require a southwestward dip for the CSZ
317 at depth. If this spatial and potentially kinematic relationship is true, we infer a depth-dependent

partitioning of the control of structural inheritance on the early development of the Lupa border fault, such that the upper sections of the fault exploited the Katuma-Wakole Terrane boundary and structures in the Katuma Terrane, and the deepest section exploited the Chisi Shear Zone.

Intra-Basinal Faulting:

The collocation and parallel trends of the KIF and CSZ suggest that the CSZ largely controlled the localization of the Karoo intra-basinal faulting (Fig. 4A and 5A). The prominence of NE-dip direction of the KIF faults (Fig. 4A) suggests that the KIF exploited the NE-dipping metamorphic fabrics along the CSZ (Fig. 2A). The confinement of the main Karoo-age rift fill between the Lupa Fault and CSZ (where present) (Fig. 5A) indicates that the KIF cluster directly influenced the first-order sediment distribution during the early phases of extension. The Karoo-age basin is widest in the northwest where the CSZ is present (CSZ rotates from NW to NNW trend, away from the Lupa Fault), further indicating the influence of the CSZ and its geometry on the extent of the early rift-related depocenter (Fig. 4A). The apparent confinement of earliest rift-related sediments also provides further age constraints on the timing of formation of the intra-basinal fault cluster. Overall, these observations indicate that the shear zone and terrane boundary represent discrete zones of inherited mechanical weakness in the crust where brittle deformation was accommodated during the early stages of continental extension.

Early-Rift Paleotopography:

The Karoo-age rift topography is likely dominated by the footwall uplift along the Lupa border fault in the northeastern basin margin (Van der Beek et al., 1998; Morley et al., 1999). However, the clustering of basement ridges along the submarine part of the CSZ, likely representative of early syn-rift erosionally-resistant topography, is consistent with observations of topographic ridges along the CSZ onshore (Figs. 1B and S2A). Elsewhere, prominent, erosionally-resistant topographic ridges define the surface expression of the Mughese Shear Zone (Kolawole et al., 2018), which appears to be a southeast continuation of the CSZ trend in the Karonga Basin (Fig. 1B). Such ridges represent elevated topographic domains that may represent important sediment sources (e.g., Gawthorpe and Leeder, 2000). Thus, the chain of ridges along the CSZ represents intra-basinal sediment-source regions near the southwestern basin margin, indicating an additional importance of the CSZ during initial sedimentation in the Rukwa Rift.

Early-Rift Distribution of Extension:

Our analyses show that within the northwestern section of the basin, Karoo-age tectonic extension was largely accommodated on both the CSZ-related intra-basinal faults (KIF) and the Lupa border fault (Figs. 4C-D); in fact, during this initial phase of extension, more strain was accommodated on intra-basinal faults than the (developing) border fault. In contrast, southeast of the CSZ termination beneath the basin (or at significantly large separation distance), extension was primarily accommodated along the Lupa border fault. These suggest that during the early phase of rifting, there was a competition for extensional strain localization between the CSZ and the Katuma-Wakole terrane boundary in the northwest. Due to the southward increase in separation between the CSZ and Katuma-Wakole/Lupa-Mbozi terrane boundaries, and the absence of CSZ

in the southeastern section of the Karoo-age basin, tectonic extension was then primarily accommodated along the Lupa Fault, which ultimately exploited the Lupa-Mbozi terrane boundary (Fig. 4C-D). The significant increase in the Lupa Fault Top-basement offset just south of the CSZ termination (Fig. 4C) also supports the dominant localization of extensional strain on the border fault in the southeastern section of the basin where the CSZ-related KIF is absent. Thus, we suggest that the CSZ strongly controlled the early-phase distribution of tectonic extension along the Rukwa Rift.

This along-rift partitioning of strain resulted in a lateral change of the overall Karoo-age rift geometry from a shallower graben in the northwest, to a deep half graben in the southeast. This along-rift change in rift geometry was previously thought to be primarily related to variation in border fault strain accommodation controlled by oblique extensional kinematics (Morley et al., 1992). Also, the obliquity of the intra-basinal faults relative to the border fault trend (Figs. 4B and 5B) has been used as a basis for inferring pull-apart and oblique extension kinematics for the rift development (Kilembe and Rosendahl, 1992; Chattopadhyay & Chakra, 2013). However, detailed structural interpretation from seismic reflection data revealed a minor component of strike-slip-related deformation along the rift (Morley et al., 1999). Thus, we here suggest that the observed obliquity of intra-basinal faults to border fault trend is primarily controlled by the focusing of extensional strain along prominent pre-existing discrete zones of basement weakness during the early phase of rifting. The geometrical alignment of the intra-basinal faults to the CSZ trend could have been influenced by local stress rotation (SHmax) into CSZ-parallel/sub-parallel trend during the early rift phase; a mechanism that has been proposed to explain the influence of weak basement fabrics on the present-day orthogonal extension kinematics along the Rukwa Rift (Morley, 2010). This resolves a long-standing controversy related to the geometrical structure and kinematics of

rift faulting in the Rukwa Rift. Elsewhere along the Rukwa Trend, farther northwest of the Rukwa Rift, the Busindi border fault of the Luama Rift exploited the NW continuation of the CSZ (Figs. 1B and 3D), demonstrating the broader influence of the CSZ on the development of the other Karoo rift segments of the Rukwa Trend. In the Tanganyika Rift, the along-rift distribution of tectonic extension is influenced by the lateral variation of the inherited crustal rheology (Wright et al., 2020), further demonstrating the strong influence of structural inheritance on the early localization and distribution of extension along continental rifts.

Post-Karoo Rift Architecture:

Geological and geophysical evidence for post-Karoo strike-slip deformation has been recorded along the Rukwa Rift (Wheeler and Karson, 1994; Delvaux et al., 2012; Heilman et al., 2019), possibly associated with a plate-scale compressional event (Daly et al., 1991; Delvaux et al., 2021). However, the analyses of seismic reflection profiles across the Rukwa Rift show that post-Karoo strike-slip or compressional deformation in the basin was very minor (Morley et al., 1999). Therefore, it is not likely that the plate-scale compressional event significantly altered the karoo-age fault patterns in the Rukwa Rift.

The CSZ and adjacent terrane boundaries continued and still continue to influence rift geometry long after the Karoo phase of extension. First, the mean trend of the rift faults, all combined (Permian to Quaternary), generally remains the same as the Karoo-age mean intra-basinal fault trend (Figs. 2Bi-ii; Morley et al., 1992; Kilembe and Rosendahl, 1992). Second, the along-strike projection of the CSZ southeast of its magnetic anomaly termination is coincident with location and orientation of the Msongano Trough, which represents a southeastward continuation of the

Rukwa Rift during the Cenozoic rifting phase (Fig. 5A). We suggest that the extension of the KIF to the CSZ termination zone already established the incipient graben of the Msongano Trough during the Karoo rifting phase (Figs. 5A and 6). We suggest that the CSZ and its colinear Mughese Shear Zone, along which the Msongano Trough developed (Fig. 5A), both constitute coupled discrete zones of weakness in the basement that accommodated the continuous lateral southeastward propagation of the KIF as a narrow graben during the post-Karoo phases of extension. Thus, the present-day bifurcation of the Rukwa Rift into the Songwe and Msongano troughs (Fig. 1C) was established during the very earliest stage of rifting. In addition, the southeastern border fault of the Rukwa Rift (Ufipa Fault; Fig. 2B) which developed in the Cenozoic, largely exploited the tectonic fabrics of the Ufipa Terrane (Heilman et al., 2019).

More broadly, in the Cenozoic Tanganyika Rift, located northwest of the Rukwa Rift (Figs. 1A-B), the rift basin is segmented (Sander and Rosendahl, 1989; Muirhead et al., 2019; Wright et al., 2020). The segmentation occurs at the proposed splay of the CSZ magnetic lineaments (Fig. 1B). The Ruzizi and East Kigoma sub-basins are separated by the northern section of the East CSZ splay, whereas the East and West Kigoma sub-basins are separated by the southern section of the East Splay, and the West Kigoma and Kalemie Sub-basins are separated by the CSZ segment extending into the Luama Rift. In essence, not only did the CSZ influence the early-phase architecture of the Karoo-age Rukwa and Luama rift basins, but also the structure of the relatively younger Tanganyika Rift. The spatial collocation of Cenozoic hydrothermal vents within different sections of the CSZ in the Tanganyika Rift (diamond symbols in Fig. 1B) highlights the deep reaches of the rift faults that exploited the basement weakness of the shear zone.

IMPLICATIONS FOR EARLY-STAGE ARCHITECTURE OF CONTINENTAL RIFT BASINS

Our study of the Rukwa Rift suggests that early-phase rift strain is significantly accommodated by intra-basinal faults, contrary to observations in some other juvenile magma-poor continental rifts (e.g., Nixon et al., 2016; Muirhead et al., 2019), but it is localized onto pre-existing structures. The early-phase strain localization in the Rukwa Rift occurred via two different styles with associated deformational mechanisms. One style (Style-1 strain localization) is the localization of a large rift fault onto a narrow discrete zone of basement weakness, such as prominent basement terrane boundaries (this study), pre-existing fault zones, and narrow ductile shear zones, in which case the structures of the weak zone and the fabrics of the adjacent basement may influence the fault geometry (Fig. 6). An example of this is the development of the Livingstone Fault in the Karonga Basin, northern Malawi Rift (Wheeler and Karson, 1989), the Thyolo border fault in the Shire Rift Zone (Wedmore et al., 2020b), and splay faulting at a terrane boundary during the Late Cretaceous extension between Zealandia and Australia (Phillips and McCaffrey, 2019b). A second style (Style-2 strain localization) is the localization of a fault cluster (or fault belt) onto a broader discrete zone of basement weakness, such as wide pre-rift shear zones or subduction suture zones (this study), in which case the individual fault strands may exploit the smaller-scale mechanical heterogeneities within the broad zone of basement weakness (Fig. 6). An example of Style-2 localization is the development of a fault cluster along the western margin of the Karonga Basin, northern Malawi Rift, where the fault cluster exploited the >15 km-wide Precambrian Mughese Shear Zone (Kolawole et al., 2018). Therefore, we hypothesize that during the earliest stages of continental rifting, strain initially localizes on pre-existing zones of crustal weakness, and the style of localization may be associated with the type of the inheritance and character of the inherited

450 structure. In addition, we note that whilst pre-existing structure may exert a strong control on strain
451 distribution and localization during the earliest phase of continental extension, the established early
452 rift template, may persist through the subsequent phases of the stretching stage of rifting (i.e., prior
453 to the necking and hyper-extension stages).

454

455 **CONCLUSIONS**

456 We investigated the distribution of strain during the earliest phase of extension in the Rukwa Rift,
457 a Phanerozoic multiphase magma-poor rift basin that developed along the trend of the Precambrian
458 Chisi Shear Zone (CSZ) and terrane boundary shear zones in East Africa.

459 Here are our main findings:

460 1) During the earliest phase of extension, although the border fault, Lupa Fault exploited the
461 colinear Katuma-Wakole and Lupa-Mbozi terrane boundaries, the CSZ facilitated the early
462 localization and development of a prominent intra-basinal fault cluster.

463 2) In the northwestern section of the rift, the presence and proximity of the CSZ and the Katuma-
464 Wakole terrane boundary facilitated a competition for strain localization between the CSZ and the
465 adjacent terrane boundary, whereas in the southeastern section where the CSZ is either absent or
466 at a significantly large distance, strain is primarily localized along the Lupa-Mbozi terrane
467 boundary.

468 3) The along-rift variation in early phase rift geometry, rift margin paleotopography, and
469 depocenter extents were largely controlled by the CSZ.

470 4) The along-rift distribution of early-phase extension was largely influenced by structural
471 inheritance, such that in the northwestern section of the rift, significant extension is accommodated

by the intra-basinal fault cluster that exploited the CSZ, whereas in the southeast, extension is largely accommodated by the Lupa border fault.

5) Two styles of early-phase strain localization in which a.) strain is localized onto a narrow discrete zone of basement weakness in the form of a large rift fault (Style-1 strain localization), and b.) strain is localized onto a broad discrete zone of basement weakness in the form of a fault cluster (Style-2 strain localization).

6) Whilst pre-existing basement structure may exert the strong control on strain distribution and localization during the earliest phase of extension, the established early rift template, may persist through the subsequent phases of the stretching stage of rifting.

Our findings offer a window into the early stages of continental extension along a young evolving magma-poor rift, where early strain is not accommodated only by border the fault as suggested by existing magma-poor early-rift models; instead, strain focuses relatively quickly on a large border fault and intra-basinal fault clusters that follow pre-existing intra-basement structures. This study reveals the influence of structural inheritance on early-phase rift geometry and along-rift partitioning of strain along magma-poor rift basins.

ACKNOWLEDGMENTS

We thank two anonymous reviewers for their insightful comments that have helped to improve the quality of our paper, and we also thank the editor, James Muirhead for handling our paper. We thank Obeid Lemna for providing useful comments on the preprint of the initial version of the manuscript uploaded on EarthArXiv. We thank the South African Council for Geoscience for providing the aeromagnetic data to EA used in this study. The aeromagnetic data is archived at http://sadc-gla.org/SADC/home.html. We have provided uninterpreted versions of the

aeromagnetic data in our supplementary document. The seismic reflection cross-section of the Rukwa Rift shown in this study (Fig. 2C) and other 2-D seismic datasets from the basin are archived in the appendix of Morley et al. (1999).

CONFLICTS OF INTEREST STATEMENT

Author Folarin Kolawole is currently employed by BP America. However, this study and the initial manuscript drafts were developed and completed during his stay at the University of Oklahoma, prior to joining BP. The remaining authors declare that the research was conducted in the absence of any commercial or financial relationships that could be construed as a potential conflict of interest.

REFERENCES CITED

Agostini, A., Bonini, M., Corti, G., Sani, F. and Mazzarini, F., 2011. Fault architecture in the Main Ethiopian Rift and comparison with experimental models: implications for rift evolution and Nubia–Somalia kinematics. Earth and Planetary Science Letters, 301(3-4), 479-492.

Baranov, V. (1957). A new method for interpretation of aeromagnetic maps: Pseudo-gravimetric anomalies. Geophysics, 22(2), 359–382.

Boniface, N. and Schenk, V., 2012. Neoproterozoic eclogites in the Paleoproterozoic Ubendian belt of Tanzania: Evidence for a Pan-African suture between the Bangweulu block and the Tanzania craton. Precambrian Research, 208, 72-89.

Boniface, N., Schenk, V. and Appel, P., 2012. Paleoproterozoic eclogites of MORB-type chemistry and three Proterozoic orogenic cycles in the Ubendian Belt (Tanzania): Evidence from monazite and zircon geochronology, and geochemistry. Precambrian Research, 192, 16-33.

Boven, A., Theunissen, K., Sklyarov, E., Klerkx, J., Melnikov, A., Mruma, A. and Punzalan, L., 1999. Timing of exhumation of a high-pressure mafic granulite terrane of the Paleoproterozoic Ubende belt (West Tanzania). Precambrian Research, 93(1), 119-137.

Buiter, S.J.H., Torsvik, T.H., 2014. A review of Wilson Cycle plate margins: a role for mantle plumes in continental break-up along sutures? Gondwana Research 26, 627–653.

Chattopadhyay, A. and Chakra, M., 2013. Influence of pre-existing pervasive fabrics on fault patterns during orthogonal and oblique rifting: an experimental approach. Marine and Petroleum Geology, 39(1), pp.74-91.

Chorowicz, J., 2005. The east African rift system. Journal of African Earth Sciences, 43(1-3), 379-410.

Christian Schiffer, Anthony G. Doré, Gillian R. Foulger, Dieter Franke, Laurent Geoffroy, Laurent Gernigon, Bob Holdsworth, Nick Kusznir, Erik Lundin, Ken McCaffrey, Alexander L. Peace, Kenni D. Petersen, Thomas B. Phillips, Randell Stephenson, Martyn S. Stoker, J. Kim Welford (2019) Structural inheritance in the North Atlantic. Earth-Science Reviews.

Claringbould, J. S., Bell, R., Jackson, C. A., Gawthorpe, R., & Odinsen, T. (2019). Complex strain partitioning and heterogeneous extension rates during early rifting in the East Shetland Basin, northern North Sea. EarthArxiv. https://doi.org/10.31223/osf.io/nbe2c

Daly, M. C. (1988). Crustal shear zones in central Africa—A kinematic approach to Proterozoic tectonics. Episodes, 11(1), 5–11.

Daly, M. C., Chorowicz, J., & Fairhead, J. D. (1989). Rift basin evolution in Africa: The influence of reactivated steep basement shear zones. Geological Society, London, Special Publications, 44(1), 309–334.

Daly, M.C., Lawrence, S.R., Kimun'a, D. and Binga, M. (1991). Late Palaeozoic deformation in central Africa: a result of distant collision?. Nature, 350(6319), pp.605-607.

Delvaux, D., 2001. Karoo rifting in western Tanzania: Precursor of Gondwana breakup. Contributions to geology and paleontology of Gondwana in honor of Helmut Wopfner: Cologne, Geological Institute, University of Cologne, 111-125.

Delvaux, D., Kervyn, F., Macheyeki, A. S., & Temu, E. B. (2012). Geodynamic significance of the TRM segment in the East African Rift (W-Tanzania): Active tectonics and paleostress in the Ufipa plateau and Rukwa basin. Journal of Structural Geology, 37, 161–180.

Delvaux, D., Maddaloni, F., Tesauro, M. and Braitenberg, C. (2021). The Congo Basin: Stratigraphy and subsurface structure defined by regional seismic reflection, refraction and well data. Global and Planetary Change, 198, p.103407.

Dewey, J., Spall, H., 1975. Pre-Mesozoic plate tectonics: how far back in Earth history can the Wilson Cycle be extended? Geology 3, 422–424.

Ebinger, C., 2005. Continental break-up: the East African perspective. Astronomy & Geophysics, 46(2), pp.2-16.

Ganbat, A., Tsujimori, T., Boniface, N., Pastor-Galán, D., Aoki, S. and Aoki, K., 2021. Crustal evolution of the Paleoproterozoic Ubendian Belt (SW Tanzania) western margin: A Central African Shield amalgamation tale. Gondwana Research, 91, pp.286-306.

Gawthorpe, R.L. and Leeder, M.R., 2008. Tectono-sedimentary evolution of active extensional basins. Basin Research, 12(3-4), pp.195-218.

Hayward, N.J. and Ebinger, C.J., 1996. Variations in the along-axis segmentation of the Afar Rift system. Tectonics, 15(2), pp.244-257.

Heilman, E., Kolawole, F., Atekwana, E. A. and Mayle, M., 2019. Controls of Basement Fabric on the Linkage of Rift Segments. Tectonics, 38(4), pp.1337-1366.

Hodgson, I., Illsley-Kemp, F., Gallacher, R.J., Keir, D., Ebinger, C.J. and Mtelela, K., 2017. Crustal structure at a young continental rift: A receiver function study from the Tanganyika Rift. Tectonics, 36(12), pp.2806-2822.

Kilembe, E.A. and Rosendahl, B.R., 1992. Structure and stratigraphy of the Rukwa rift. In: C.J. Ebinger, H.K. Gupta and 1.0. Nyambok (Editors), Seismology and Related Sciences in Africa. Tectonophysics, 209: 143-158.s

Klerkx, J., Theunissen, K. and Delvaux, D., 1998. Persistent fault controlled basin formation since the Proterozoic along the Western Branch of the East African Rift. Journal of African Earth Sciences, 26(3), pp.347-361.

Kolawole, F., Atekwana, E.A., Laó-Dávila, D.A., Abdelsalam, M.G., Chindandali, P.R., Salima, J. and Kalindekafe, L., 2018. Active deformation of Malawi rift's north basin Hinge zone

575 modulated by reactivation of preexisting Precambrian Shear zone fabric. Tectonics, 37(3), 683-
576 704.

577 Kolawole, F., Atekwana, E.A., Malloy, S., Stamps, D.S., Grandin, R., Abdelsalam, M.G., Leseane,
578 K. and Shemang, E.M., 2017. Aeromagnetic, gravity, and Differential Interferometric Synthetic
579 Aperture Radar analyses reveal the causative fault of the 3 April 2017 Mw 6.5 Moiyabana,
580 Botswana, earthquake. Geophysical Research Letters, 44(17), pp.8837-8846.

581 Lee, H., Fischer, T.P., Muirhead, J.D., Ebinger, C.J., Kattenhorn, S.A., Sharp, Z.D., Kianji, G.,
582 Takahataf, N., Sano, Y., 2017. Incipient rifting accompanied by the release of subcontinental
583 lithospheric mantle volatiles in the Magadi and Natron basin, East Africa. J. Volcanol. Geotherm.
584 Res.346, 118–133.

585 Lemna, O.S., Stephenson, R. and Cornwell, D.G., 2019. The role of pre-existing Precambrian
586 structures in the development of Rukwa Rift Basin, southwest Tanzania. Journal of African Earth
587 Sciences, 150, 607-625.

588 Lenoir, J.L., Liégeois, J.P., Theunissen, K. and Klerkx, J., 1994. The Palaeoproterozoic Ubendian
589 shear belt in Tanzania: geochronology and structure. Journal of African Earth Sciences, 19(3),
590 pp.169-184.

591 Muirhead, J.D., Kattenhorn, S.A., Lee, H., Mana, S., Turrin, B.D., Fischer, T.P., Kianji, G., Dindi,
592 E., Stamps, D.S., 2016. Evolution of upper crustal faulting assisted by magmatic volatile release
593 during early-stage continental rift development in the East African Rift. Geosphere, 12, 1670–
594 1700.

595 Muirhead, J.D., Wright, L.J. and Scholz, C.A., 2019. Rift evolution in regions of low magma input
596 in East Africa. Earth and Planetary Science Letters, 506, pp.332-346.

597 Morley, C.K., 2010. Stress re-orientation along zones of weak fabrics in rifts: An explanation for
598 pure extension in 'oblique' rift segments?. Earth and Planetary Science Letters, 297(3-4), pp.667-
599 673.

600 Morley, C.K., Cunningham, S.M., Harper, R.M. and Wescott, W.A., 1992. Geology and
601 geophysics of the Rukwa rift, East Africa. Tectonics, 11(1), pp.69-81.

602 Morley, C.K., Wescott, W.A., Harper, R.M. and Cunningham, S.M., 1999. Geology and
603 geophysics of the Rukwa Rift. Geoscience of Rift Systems-Evolution of East Africa. AAPG
604 Studies in Geology, 44, pp.91-110.

605 Naliboff, J.B., Buiter, S.J., Péron-Pinvidic, G., Osmundsen, P.T. and Tetreault, J., 2017. Complex
606 fault interaction controls continental rifting. Nature communications, 8(1), pp.1-9.

607 Nixon, C.W., McNeill, L.C., Bull, J.M., Bell, R.E., Gawthorpe, R.L., Henstock, T.J.,
608 Christodoulou, D., Ford, M., Taylor, B., Sakellariou, D. and Ferentinos, G., 2016. Rapid
609 spatiotemporal variations in rift structure during development of the Corinth Rift, central Greece.
610 Tectonics, 35(5), pp.1225-1248.

Osagiede, E.E., Rotevatn, A., Gawthorpe, R., Kristensen, T.B., Jackson, C.A. and Marsh, N., 2020. Pre-existing intra-basement shear zones influence growth and geometry of non-colinear normal faults, western Utsira High–Heimdal Terrace, North Sea. Journal of Structural Geology, 130, p.103908.

Phillips, T.B., Fazlikhani, H., Gawthorpe, R.L., Fossen, H., Jackson, C.A.L., Bell, R.E., Faleide, J.I. and Rotevatn, A., 2019a. The Influence of Structural Inheritance and Multiphase Extension on Rift Development, the Northern North Sea. Tectonics, 38.

Phillips, T.B. and McCaffrey, K.J., 2019b. Terrane Boundary Reactivation, Barriers to Lateral Fault Propagation and Reactivated Fabrics: Rifting Across the Median Batholith Zone, Great South Basin, New Zealand. Tectonics, 38(11), 4027-4053.

Ragon, T., Nutz, A., Schuster, M., Ghienne, J.F., Ruffet, G. and Rubino, J.L., 2019. Evolution of the northern Turkana Depression (East African Rift System, Kenya) during the Cenozoic rifting: New insights from the Ekitale Basin (28-25.5 Ma). Geological Journal, 54(6), pp.3468-3488.

Roberts, E.M., O'Connor, P.M., Stevens, N.J., Gottfried, M.D., Jinnah, Z.A., Ngasala, S., Choh, A.M. and Armstrong, R.A., 2010. Sedimentology and depositional environments of the Red Sandstone Group, Rukwa Rift Basin, southwestern Tanzania: New insight into Cretaceous and Paleogene terrestrial ecosystems and tectonics in sub-equatorial Africa. Journal of African Earth Sciences, 57(3), pp.179-212.

Roberts, E.M., Stevens, N.J., O'Connor, P.M., Dirks, P.H.G.M., Gottfried, M.D., Clyde, W.C., Armstrong, R.A., Kemp, A.I.S. and Hemming, S., 2012. Initiation of the western branch of the East African Rift coeval with the eastern branch. Nature Geoscience, 5(4), pp.289-294.

Salem, A., Williams, S., Fairhead, J. D., Smith, R., & Ravat, D. (2007). Interpretation of magnetic data using tilt-angle derivatives. Geophysics, 73(1), L1–L10.

Sklyarov, E.V., Theunissen, K., Melnikov, A.I., Klerkx, J., Gladkochub, D.P., Mruma, A., 1998. Paleoproterozoic eclogites and garnet pyroxenites of the Ubende Belt (Tanzania). Schweizerische Mineralogische Petrographische Mitteilungen 78, 257–271.

Smirnov, V., Pentelkov, V., Tolochko, V., Trifan, M., Zhukov, S., 1973. Geology and minerals of the central part of the western rift. Tech. rep., Mineral and Resource Division, Dodoma, Tanzania. Unpublished report of the geological mapping.

Theunissen, K., Klerkx, J., Melnikov, A., & Mruma, A. (1996). Mechanisms of inheritance of rift faulting in the western branch of the East African Rift, Tanzania. Tectonics, 15(4), 776–790.

Van der Beek, P., Mbede, E., Andriessen, P. and Delvaux, D., 1998. Denudation history of the Malawi and Rukwa Rift flanks (East African Rift System) from apatite fission track thermochronology. Journal of African Earth Sciences, 26(3), pp.363-385.

Versfelt, J.W. (2009), South Atlantic margin rift basin asymmetry and implications for pre-salt exploration. International Petroleum Technology Conference (IPTC) paper 13833, Doha, Qatar.

Wang, L., Maestrelli, D., Corti, G., Zou, Y. and Shen, C., 2021. Normal fault reactivation during multiphase extension: Analogue models and application to the Turkana depression, East Africa. Tectonophysics, 811, p.228870.

Wedmore, L.N., Biggs, J., Williams, J.N., Fagereng, Å., Dulanya, Z., Mphepo, F. and Mdala, H., 2020a. Active fault scarps in southern Malawi and their implications for the distribution of strain in incipient continental rifts. Tectonics, 39(3), p.e2019TC005834.

Wedmore, L.N., Williams, J.N., Biggs, J., Fagereng, Å., Mphepo, F., Dulanya, Z., Willoughby, J., Mdala, H. and Adams, B.A., 2020b. Structural inheritance and border fault reactivation during active early-stage rifting along the Thyolo fault, Malawi. Journal of Structural Geology, 139, 104097.

Wheeler, W.H. and Karson, J.A., 1989. Structure and kinematics of the Livingstone Mountains border fault zone, Nyasa (Malawi) Rift, southwestern Tanzania. Journal of African Earth Sciences (and the Middle East), 8(2-4), 393-413.

Wheeler, W.H. and Karson, J.A., 1994. Extension and subsidence adjacent to a" weak" continental transform: An example from the Rukwa rift, East Africa. Geology, 22(7), 625-628.

Wilson, J.T., 1966. Did the Atlantic close and then re-open? Nature 211, 676–681.

Wright, L. J. M., Muirhead, J. D., & Scholz, C. A. (2020). Spatiotemporal variations in upper crustal extension across the different basement terranes of the Lake Tanganyika Rift, East Africa. Tectonics, 39, e2019TC006019.

FIGURES

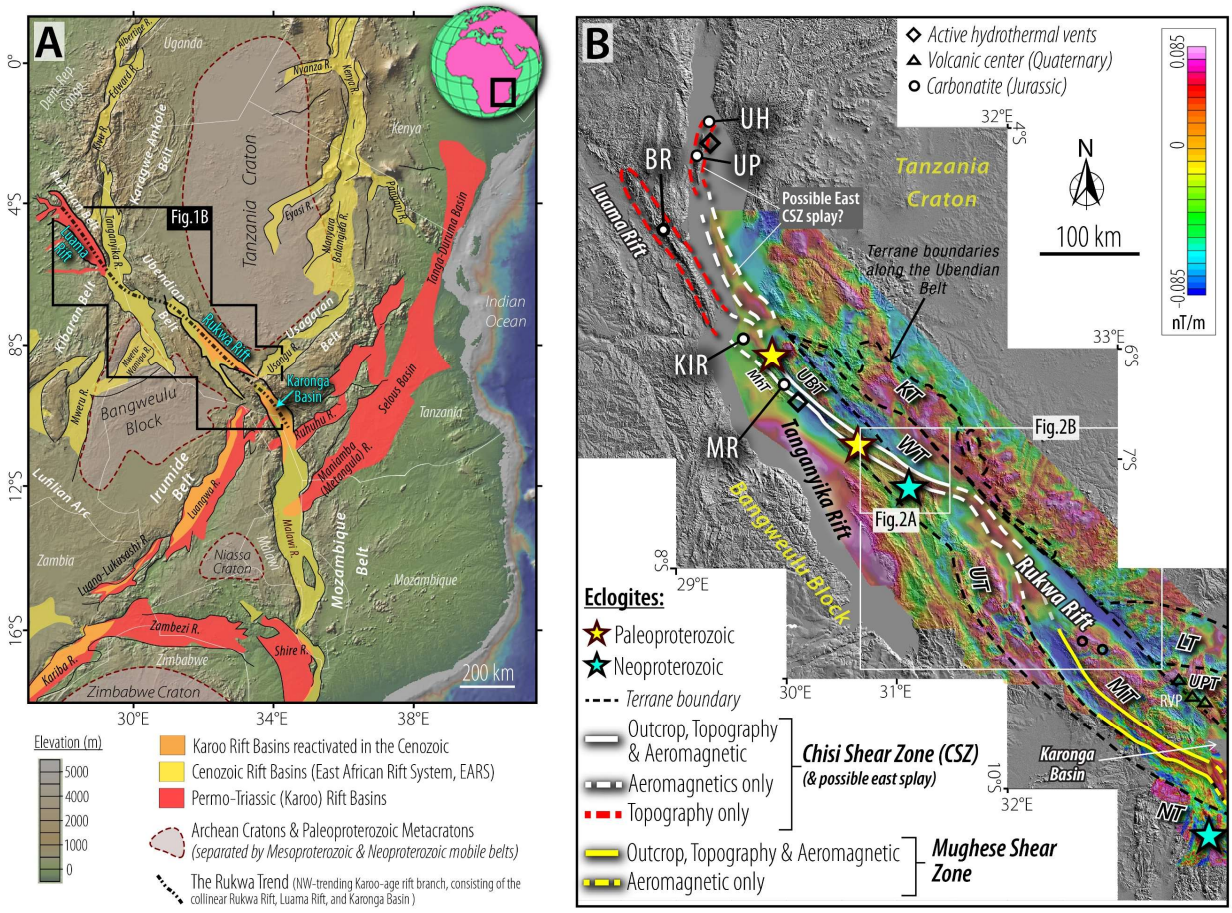

Figure 1. A: Map of east Africa showing the Permo-Triassic (i.e., Karoo rift system) rift segments, and the currently active rift segments (i.e., East African Rift System). **B:** Shuttle Radar Topography Mission (SRTM) Digital Elevation Model (DEM) hillshade covering the Rukwa Rift Trend, overlaid with the vertical derivative aeromagnetic of SW Tanzania. Black dashed lines represent boundaries of the Precambrian terranes of the Rukwa Rift Trend (after Daly, 1988; Lenoir et al., 1994; Delvaux et al., 2012; Lemna et al., 2018; Heilman et al., 2019). Locations of Proterozoic eclogites in the Ubendian Belt are from Boniface et al. (2012) and Boniface and Schenk (2012). Locations of hydrothermal vents and Mesozoic-Cenozoic igneous centers (volcanics and carbonatites) are obtained from Hodgson et al. (2017). See uninterpreted aeromagnetic and hillshade maps in supplementary figures 1 and 2. Geomorphic features: BR (Busindi Ridge), KIR (Kavala Island Ridge), MR (Mahale Ridge), UP (Ubwari Peninsula), UH (Ubwari Horst). Terranes of the Ubendian Belt: KT (Katuma Terrane), LT (Lupa Terrane), MT (Mbozi Terrane), MhT (Mahale Terrane), RVP (Rungwe Volcanic Province), UBT (Ubende Terrane), UPT (Upangwa Terrane), UT (Ufipa Terrane), WT (Wakole Terrane).

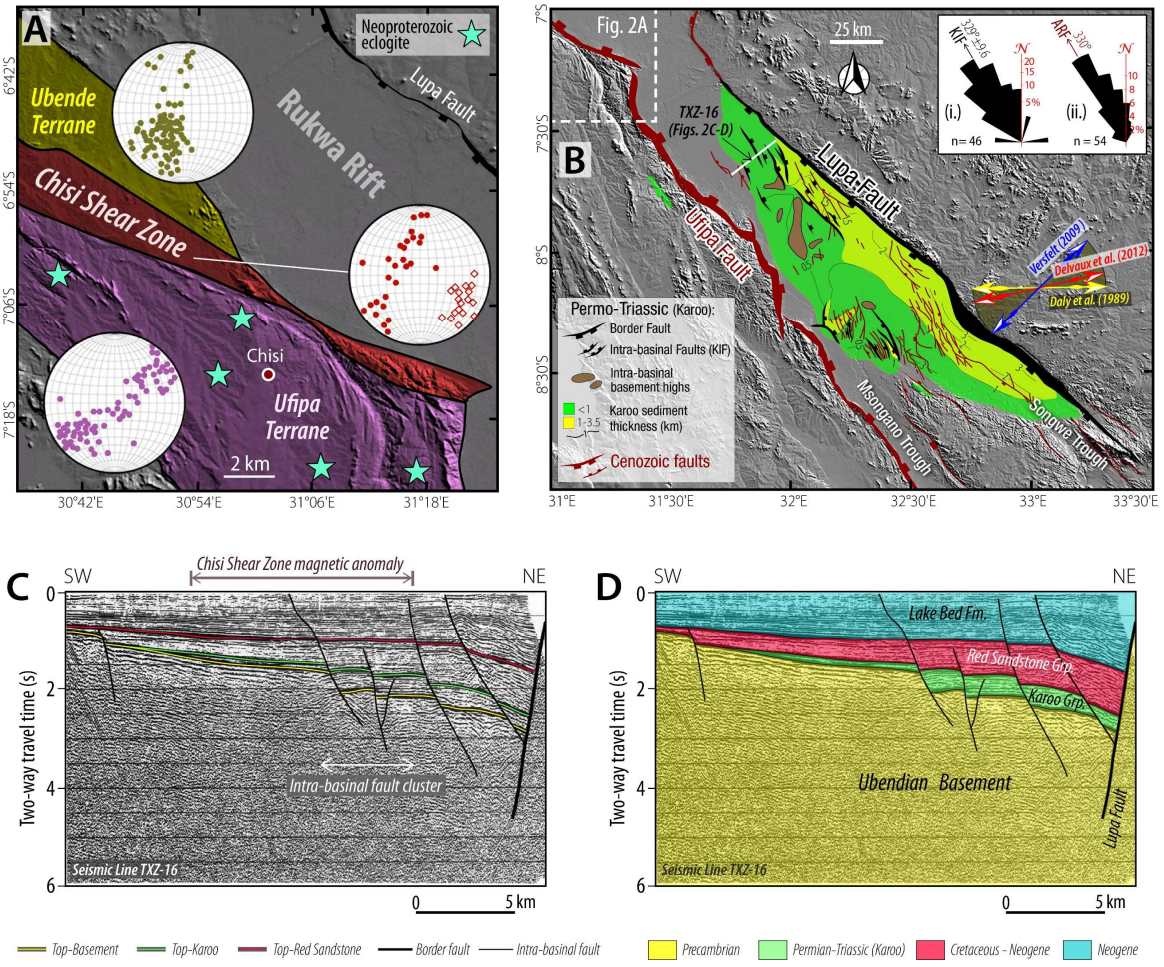

Figure 2. A: Satellite digital elevation model (DEM) hillshade of the NW Rukwa Rift shoulder (see Figs. 1B and 2B for location) showing the Precambrian Chisi Shear Zone exposure and its bounding basement terranes. The plots of equal area stereographic projection (lower hemisphere) show the poles to planes of gneissic foliation (filled circles), and poles of mineral elongation lineation and some fold axes of asymmetric intrafolial folds (diamonds in the Chisi Shear Zone stereonet) measured in field outcrops (from Boven et al., 1999). These structures represent the metamorphic basement fabrics of the basement. Locations of Neoproterozoic eclogites in the Chisi area are from Boniface and Schenk (2012). **B:** Map of the Rukwa Rift showing the interpreted Karoo and post-Karoo structural elements (structural elements are from Morley et al., 1992, 1999). Arrows represent the previously published inferred Karoo extension directions. *Inset:* Frequency-azimuth distribution plot for (*i.)* Karoo-age (Permo-Triassic) intra-basinal faults (KIF) with black arrow indicating their mean trend and standard error (measured in this study), and *(ii.)* All (Permian to Quaternary) Rukwa Rift faults (ARF) with their mean trend shown as brown arrow (digitized from Morley et al., 1992). **C - D:** 2-D seismic reflection profile line TXZ-16 and interpretation (modified from Morley et al., 1999; see location in Fig. 2B) showing the major stratigraphic boundary horizons, the Lupa border fault, and intra-basinal faults.

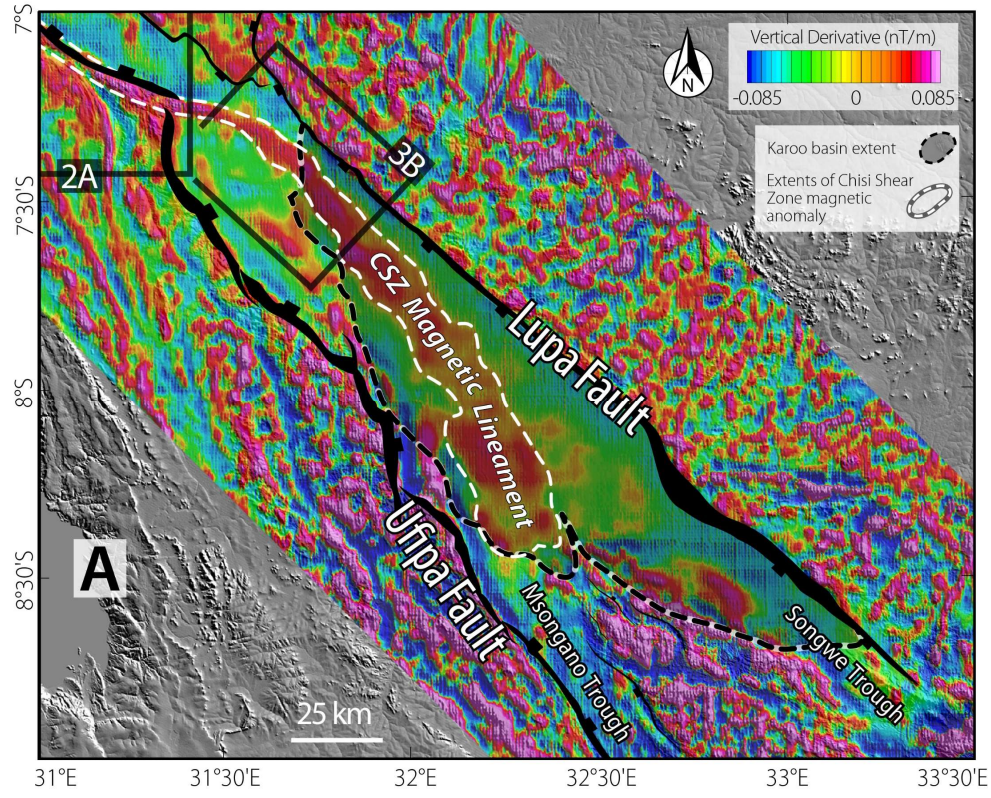
Vertical Derivative (nT/m)
-0.085
0
0.085
Karoo basin extent
Extents of Chisi Shear Zone magnetic anomaly
2A
3B
CSZ Magnetic Lineament
Lupa Fault
Ufipa Fault
Msongano Trough
Songwe Trough
A
25 km
7°S
7°30'S
8°S
8°30'S
31°E
31°30'E
32°E
32°30'E
33°E
33°30'E

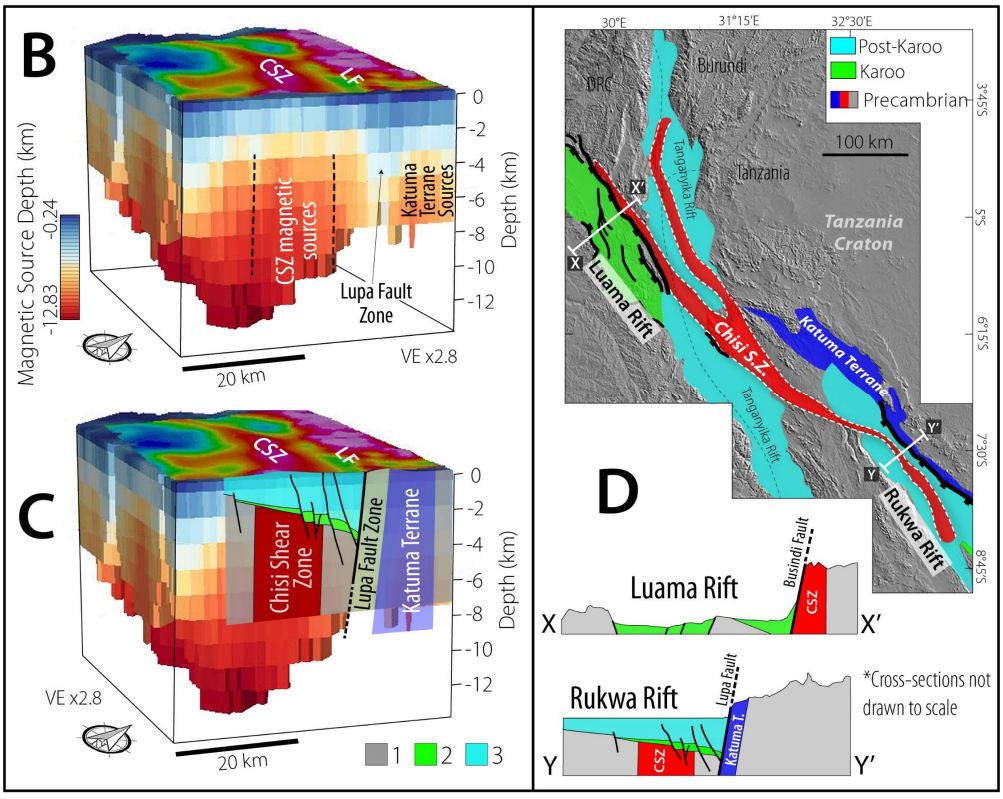
B
CSZ
LF
CSZ magnetic sources
Katuma Terrane Sources
Lupa Fault Zone
Magnetic Source Depth (km)
-0.24
-12.83
Depth (km)
0
-2
-4
-6
-8
-10
-12
VE x2.8
20 km
C
CSZ
LF
Chisi Shear Zone
Lupa Fault Zone
Katuma Terrane
Depth (km)
VE x2.8
20 km
1
2
3
30°E
31°15'E
32°30'E
DRC
Burundi
Tanzania
Post-Karoo
Karoo
Precambrian
100 km
Tanganyika Rift
Tanzania Craton
Luama Rift
Chisi S.Z.
Katuma Terrane
Rukwa Rift
X
X'
Y
Y'
D
Luama Rift
Busindi Fault
CSZ
Rukwa Rift
Lupa Fault
Katuma T.
*Cross-sections not drawn to scale

Figure 3. A: Vertical derivative of the aeromagnetic grid overlaid on satellite Digital Elevation Model (DEM) hillshade, showing the rift border faults, rift shoulder basement fabrics and the aeromagnetic signature of the Chisi Shear Zone (CSZ) along the rift axis. See uninterpreted aeromagnetic maps in supplementary figure 1. **B:** 3-D gridded block of the Source Parameter Imaging (SPI) solutions from the transform of the aeromagnetic grid, showing the subsurface extents and geometry of CSZ and the shallower Katuma Terrane magnetic sources. **C:** 3-D gridded block overlaid with interpretations of the rift faults and simplified stratigraphy (interpretations from 2-D seismic line TXZ-16 of Morley et al., 1999 shown in Fig. 2C). Stratigraphic units shown: 1 = Precambrian basement), 2 = Permo-Triassic (Karoo Grp.) sequences, 3 = Post-Karoo sequences i.e., Red Bed Grp. and Lake Bed Fm.). **D:** Regional satellite DEM hillshade showing the >600 km extent of the CSZ and its relationships with the Rukwa and Luama segments of the Rukwa Trend. Cross-sections are based on satellite DEM (Luama Rift), and satellite DEM, aeromagnetics, and 2-D seismic data interpretation (Rukwa Rift).

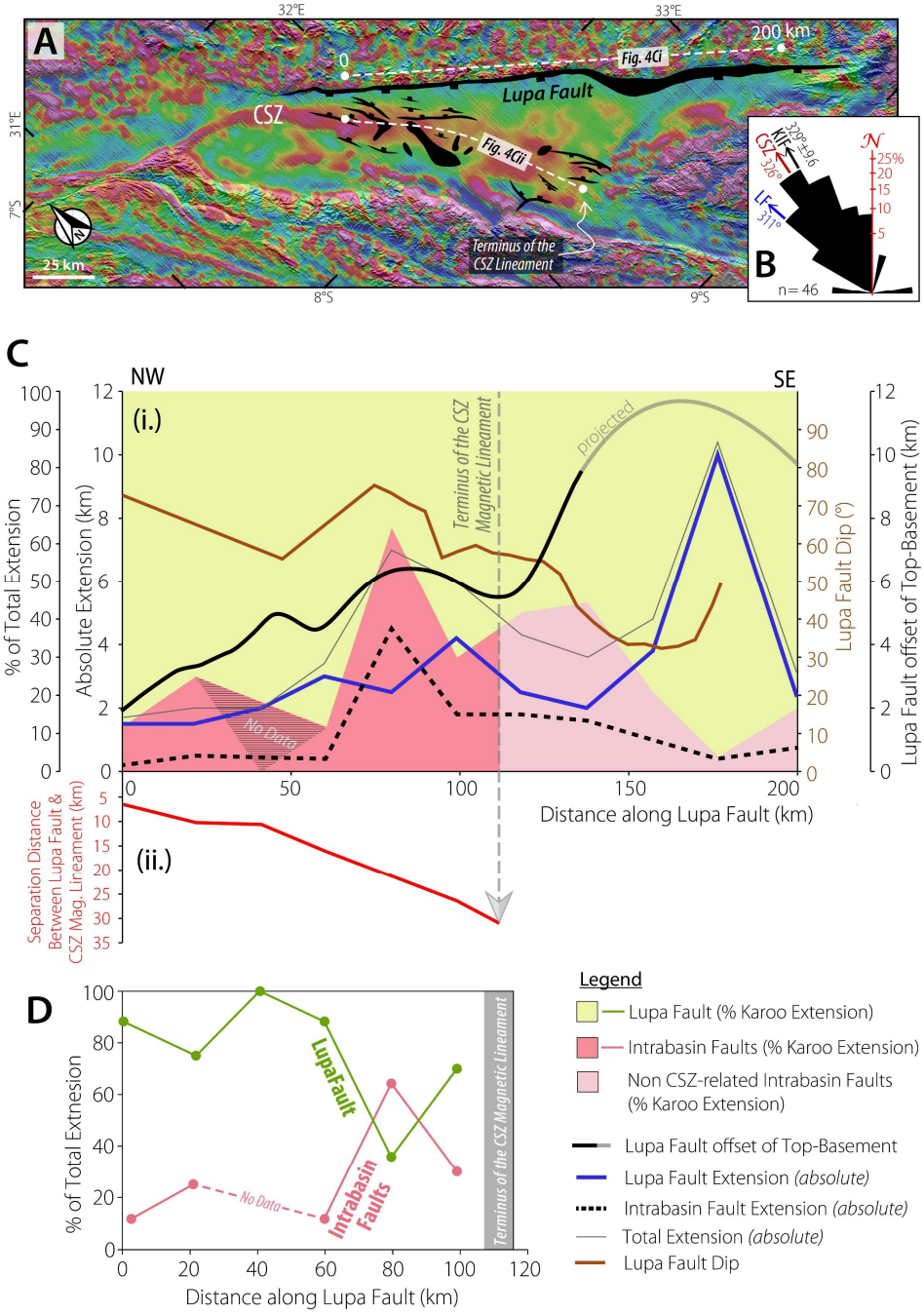

Figure 4. A: Map of vertical derivative of the aeromagnetic grid overlaid on satellite DEM hillshade, showing the section of the Rukwa Rift (white dashed lines) along which, the measurements plotted in Figures 4C-D were taken. **B:** Frequency-azimuth distribution of the Karoo-age intra-basinal faults (KIF; measured in this study). CSZ = Chisi Shear Zone, LF = Lupa Fault. Arrows represent the mean trend of the associated structure. **C:** Plot showing along-rift distribution of (i.) line-length measurement of the Top-Karoo surface as estimates of Karoo-age tectonic extension (for the Lupa and intra-basinal faults), Lupa Fault dip angle, and Top-Basement offset along the Lupa Fault, and (ii.) lateral separation distance between the CSZ and the Lupa Fault. **D:** Plot showing the along-rift variation of % total Karoo-age extension accommodated by

the Lupa Fault and the intra-basinal faults up till the CSZ termination (displayed as stacked area plot in Fig. 4C).

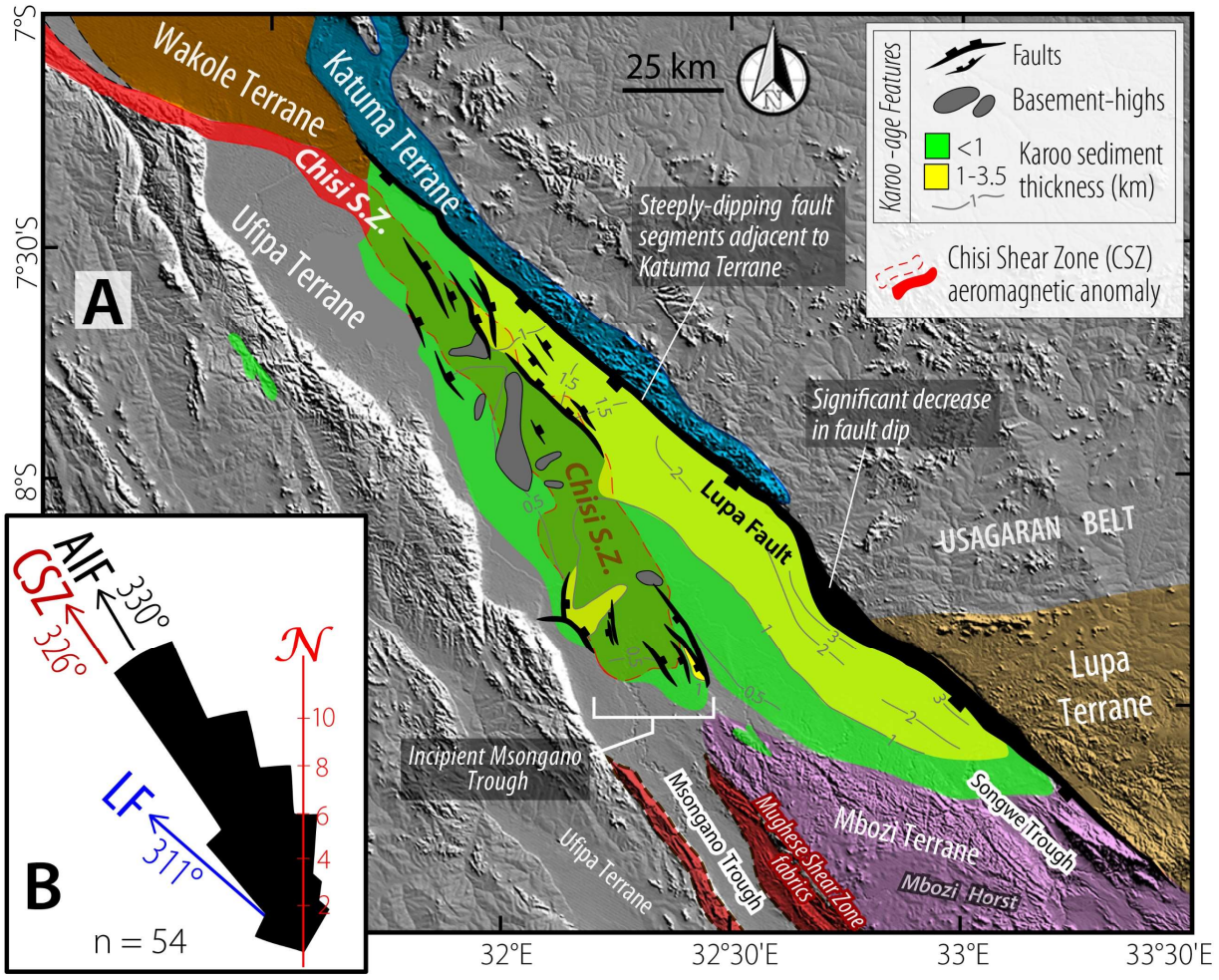

Figure 5. A: Satellite DEM hillshade of the Rukwa Rift, overlaid with the Karoo structural features (faults and basement ridges), Karoo isopach map (from Morley et al., 1992, 1999), Chisi Shear Zone magnetic anomaly, and the relevant surrounding basement terranes. **B:** Frequency-azimuth distribution of all the faults (Permian-Quaternary) in the Rukwa Rift (digitized from Morley et al., 1992). ARF = "All Rukwa Rift faults" and black arrow showing their mean trend; LF = "Lupa Fault" and blue arrow showing its approximate trend; CSZ = "Chisi Shear Zone" and brown arrow showing its approximate trend within the rift axis.

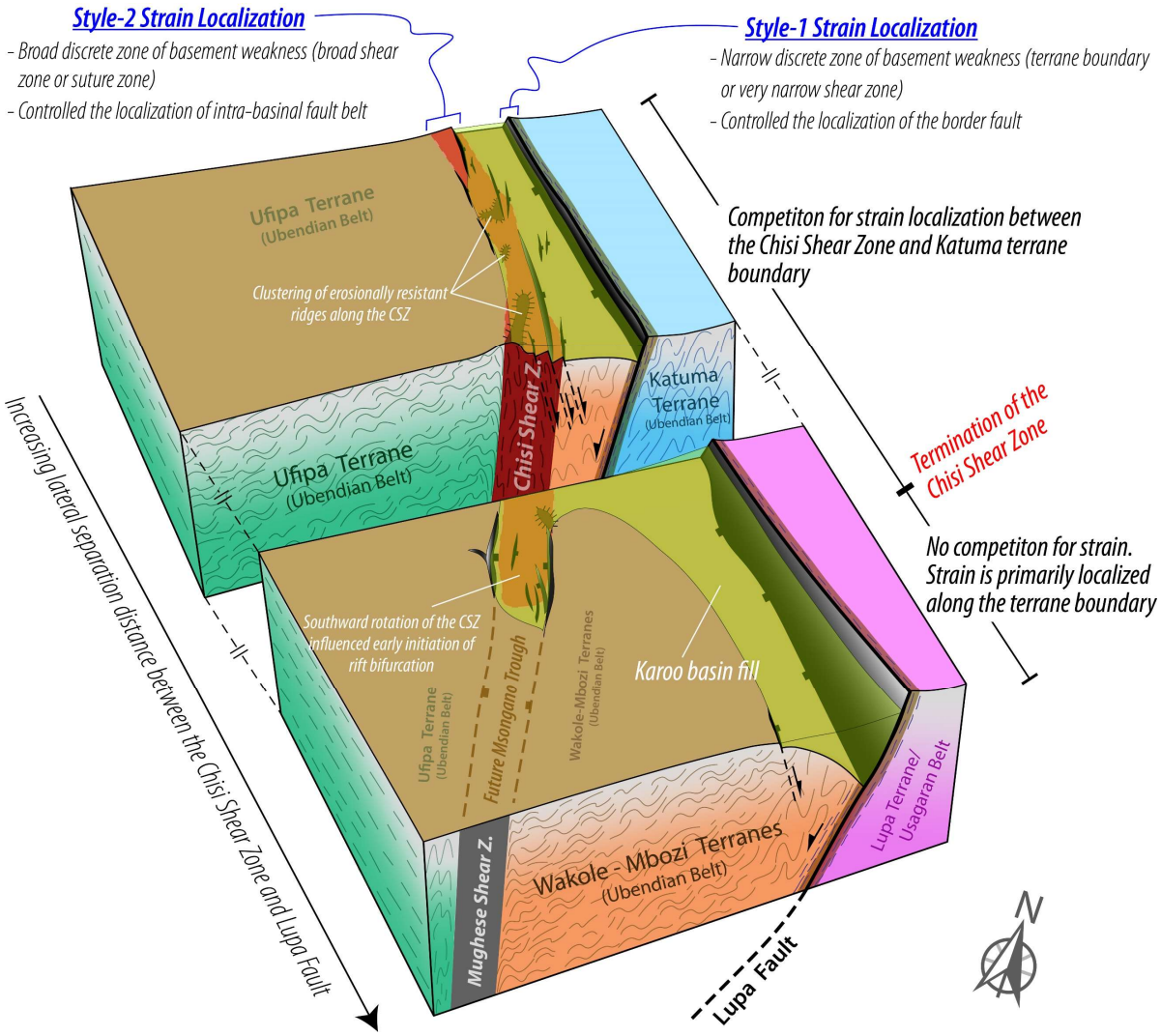

Figure 6. Cartoon illustrating some of the key observations in this study, showing how the structure of discrete zones of basement weakness influenced strain localization styles and along-rift distribution of extension during the early phase of tectonic extension in the Rukwa Rift.